

# TEMPERATURES, DENSITIES, AND WINDS IN THE HIGH LATITUDE (78°N) MESOSPHERE

F.-J. Lübken<sup>1</sup> and A. Müllemann<sup>1</sup>

<sup>1</sup>*Institute of Atmospheric Physics (IAP), Schloss-Str. 6, 18225 Kühlungsborn, Germany*

## ABSTRACT

A field campaign called ROMA (“Rocket borne Observations in the Middle Atmosphere”) was conducted in 2001 close to Longyearbyen (Spitsbergen, 78°N) with temperature, density, and wind measurements by meteorological rockets and ground-based detection of noctilucent clouds (NLC) by lidar and polar mesosphere summer echoes (PMSE) by radar. A summary of the temperature data has been published recently [Lübken and Müllemann, 2003]. Here we present a detailed comparison of temperatures and densities with empirical models (CIRA, MSIS) and with measurements at other latitudes. We also present falling sphere winds. It is very cold in the upper mesosphere during the summer season, cold enough for water ice particles to exist, i. e., the degree of saturation is larger than unity assuming reasonable [H<sub>2</sub>O] values. Generally, PMSE and NLC are found at altitudes with super-saturation. There are striking differences and similarities between temperatures and densities at Longyearbyen, empirical reference models, and measurements at other latitudes, respectively. For example, around the mesopause in summer, temperatures are smaller by 6–9 K in Longyearbyen compared to Andøya (69°N). Much larger differences are observed relative to CIRA: temperatures are smaller by up to 20 K and mass densities in the upper mesosphere are almost 50% smaller compared to CIRA-1986. In the lower and middle atmosphere, temperatures and densities are very similar to values at Andøya and to empirical models. Zonal winds are westward in the mesosphere and generally agree with CIRA-1986, both in direction and magnitude. Meridional winds are smaller than zonal winds.

## INTRODUCTION

The high latitude summer mesosphere (HLSM) is one of the most intriguing regions of the terrestrial atmosphere since temperatures deviate by several tens of Kelvin from radiative equilibrium values. This implies that dynamical processes must play an important role in governing the thermal structure at these heights. The generally accepted concept of this dynamical control is based on gravity waves which propagate from the troposphere into the mesosphere where they deposit momentum and energy when they break due to convective or Kelvin-Helmholtz instabilities [see for example Lindzen, 1981]. Many details of this coupling and the energy budget in general are not well understood. For example, in situ measurements by rockets have shown that heating by turbulent dissipation of energy is largest at the summer mesopause, i. e., exactly at altitudes where we observe the lowest temperatures in the entire atmosphere [Lübken *et al.*, 2002b]. In the HLSM we find several layered phenomena which are related to these very low temperatures. Examples of such layers are “noctilucent clouds” (NLC) and “polar mesosphere summer echoes” (PMSE). Reviews on these phenomena are presented elsewhere [Gadsden and Schröder, 1989; Cho and Röttger, 1997]. Recent progress in modeling has explained the main features of PMSE in terms of electron diffusivity reduction by charged ice particles and neutral dynamics [Rapp and Lübken, 2003].

Experimental investigations in the HLSM are difficult since optical methods are hampered by permanent daylight conditions whereas in situ measurements are relatively sparse. In this paper we report on first temperature measurements in the HLSM at very high latitudes (78°N) performed by meteorological rockets

in 2001. First results have been presented in *Lübken and Müllemann* [2003]. A field campaign called ROMA (“Rocket borne Observations in the Middle Atmosphere”) was conducted in summer 2001 close to Longyearbyen (78°15’N,15°24’E) on the Arctic island Spitsbergen which is part of the archipelago Svalbard. In this paper we concentrate on results from falling spheres, in particular on temperatures, densities, and horizontal winds. We present a detailed comparison with measurements at 69°N and with empirical model atmospheres.

A potassium lidar and a VHF radar were also available during ROMA at Longyearbyen and measured NLC and PMSE, respectively. These ground based instruments are only ~15 km apart from each other. The falling sphere measurements were made at a horizontal distance of approximately 40–50 km from these instruments. A first intercomparison of the thermal structure and the appearance of NLC and PMSE is presented in *Lübken et al.* [2002a].

## MEASUREMENTS DURING THE ROMA CAMPAIGN

### Meteorological Rockets

A series of meteorological rockets were launched in the period July 16 to September 14, 2001, from a mobile launcher installed close to Longyearbyen. The temperature, density, and wind measurements reported here were performed employing the “falling sphere” (FS) technique. 24 falling spheres were launched successfully in a regular interval of approximately 3 days.. The falling sphere technique is described in detail elsewhere [*Schmidlin*, 1991; *Lübken et al.*, 1994]. This technique gives densities and horizontal winds in an altitude range from approximately 95 to 30 km. Temperatures are obtained by integrating the density profile assuming hydrostatic equilibrium. The temperature at the top of the FS profile (‘start temperature’  $T_o$ ) has to be taken from independent measurements or from a model. We have taken  $T_o$  from a preliminary data analysis of the potassium lidar measurements (described below) which gave smoothed and interpolated temperature profiles for the entire ROMA period (*Höffner*, private communication). The availability of lidar temperatures significantly improves the FS accuracy in the upper part of the profiles since it reduces the uncertainty about the start temperature. The height-dependent sphere reaction time-constant causes a smoothing of the density, temperature, and wind profiles. The smallest scales detectable are typically 8, 3, and 0.8 km at 85, 60, and 40 km, respectively. The uncertainty of the temperatures is typically 7, 3, and 1.5 K at 90, 80, and 70 km. We note that the FS technique shows excellent overall agreement with entirely different rocket borne temperature measurements with much better altitude resolution [*Rapp et al.*, 2001, 2002]. In particular the mean mesopause structure is nicely reproduced.

### Ground-based

Noctilucent clouds and atmospheric temperatures are observed by the potassium lidar mentioned above. This technique deduces atmospheric temperatures in the potassium layer from measurements of the spectral width of the Doppler broadened K-D<sub>1</sub> resonance line at 769.9 nm [*von Zahn and Höffner*, 1996]. The lidar temperatures are available at 15 minutes and 1 km interval. The uncertainty of the K lidar temperatures is typically a few Kelvin. An overview of NLC data obtained during this campaign is presented in *Höffner et al.* [2003].

The SOUSY Svalbard VHF radar (SSR), a project of the Max-Planck-Institut fuer Aeronomie was operated in summer 2001 as an integral part of the ROMA campaign. First results regarding the seasonal and height variation of PMSE at Spitsbergen are published in *Rüster et al.* [2001]. A detailed comparison of PMSE obtained during ROMA with NLC and FS temperatures will be presented in the future.

### Measurements

In Figure 1 the temperature profile from flight ROFS07 launched on July 31 at 09:00 UT is shown together with a reference profile taken from a climatology obtained from FS at Andøya, 69°N [*Lübken*, 1999], hereafter referred to as “FJL-JGR99”. As can be seen from Figure 1 (left panel) temperatures are very low in the upper mesosphere, typically less than 150 K. The mesopause temperature and altitude are 138.2 K and 92.4 km, respectively. As is shown in more detail below, the summer mesopause at 78°N in general is somewhat colder and higher compared to the 69°N climatology [see *Lübken and Müllemann*, 2003, for more details]. In Figure 1 we also show the frost point temperatures  $T_{frost}$  using two different water vapor mixing ratio profiles: a) 5 ppmv, constant with altitude, and b) the [H<sub>2</sub>O] values from the theoretical model of

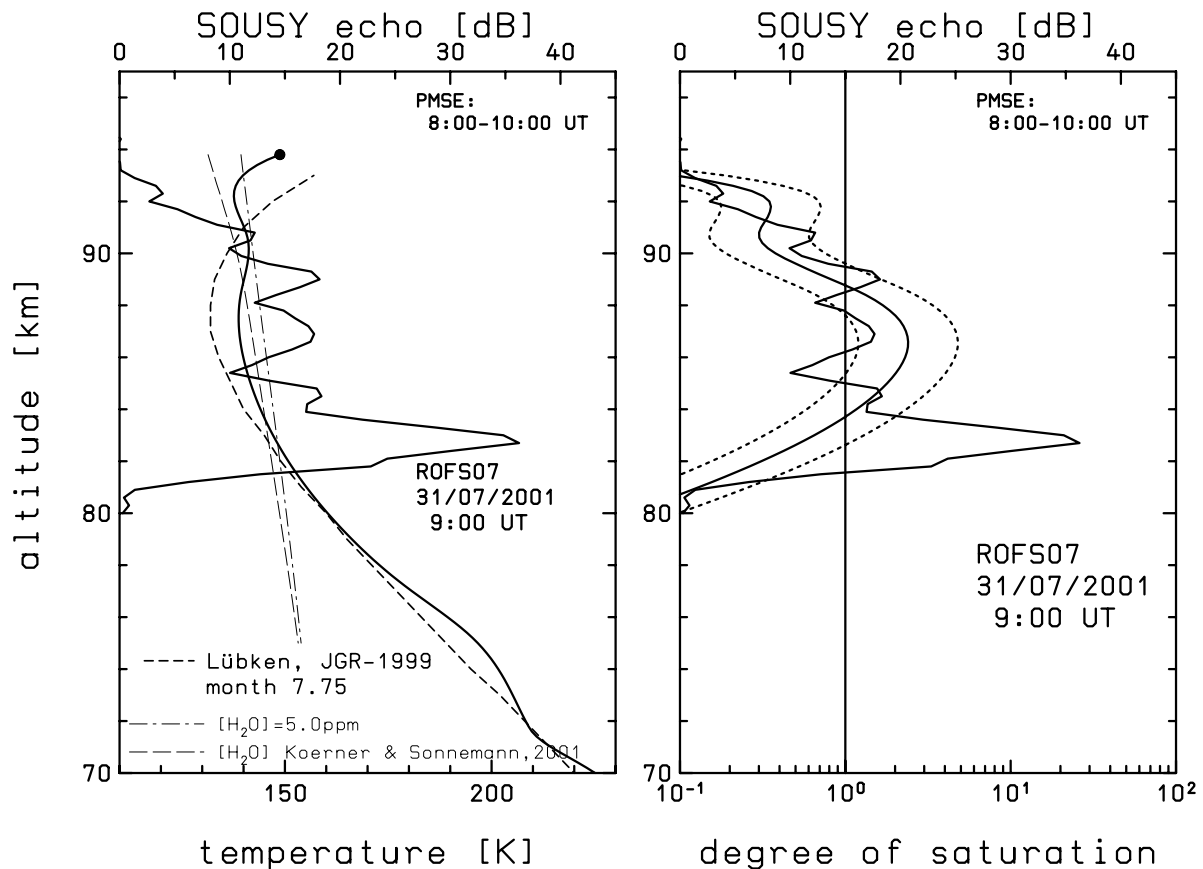


Fig. 1. Falling sphere flight ROFS07: Temperature (left panel) and degree of saturation (right panel). The flight labels, launch dates, and times are indicated in the inlet. For comparison the temperature profile from the climatology at  $69^\circ\text{N}$  (FJL-JGR99) is shown (thick dashed line). The thin lines in the left panel indicate frost point temperatures  $T_{frost}$  using model water vapor mixing ratios from *Körner and Sonnemann* [2001] (K&S) and a mixing ratio of 5 ppmv independent of altitude. The PMSE echo is shown in both panels (upper abscissa) averaged for  $\pm 1$  h around the rocket launch and is taken from *Röttger* [private communication, 2002]. The degree of saturation (right panel) is calculated assuming  $[\text{H}_2\text{O}]$  values from K&S, also for values increased (decreased) by a factor of 2 (dashed lines).

*Körner and Sonnemann* [2001] (K&S). As can be seen from Figure 1 the temperatures for flight ROFS07 are smaller than  $T_{frost}$  in an altitude range around 87 km indicating that it is cold enough at these heights for ice particles to grow or exist. In the right panel of Figure 1 we show the degree of saturation derived from the FS temperatures of flight ROFS07, assuming  $[\text{H}_2\text{O}]$  from K&S, and also water vapor concentrations which are smaller and larger by a factor of 2, respectively. A PMSE was observed during the ROFS07 flight which is also shown in Figure 1. In general, the PMSE occurs at altitudes where the degree of saturation exceeds (or is close to) super-saturation, i. e., where  $T_{atm} < T_{frost}$ . The altitude profiles of PMSE and S show a very similar behaviour. The upper and lower part of the PMSE are located in a region with under-saturation ( $S < 1$ ), i. e., where no ice particles (yet no PMSE) should exist. We attribute this apparent discrepancy to temporal and spatial variability, and to the combined uncertainty of  $[\text{H}_2\text{O}]$  and temperatures. We note that there might be small scale temperature structures in connection with PMSE that are smaller than the height resolution of the falling sphere technique [*Lübken et al.*, 2002b]. We conclude that there exists a close correlation between low temperatures and PMSE. When comparing PMSE and S it should be noted that neutral dynamics (turbulence) is also required to generate PMSE [*Rapp and Lübken*, 2003].

A summary of the temperatures from all FS flights is presented in *Lübken and Müllemann* [2003] (Plate 1). The density and temperature tables presented in that publication can be downloaded from the IAP web page ([www.iap-kborn.de](http://www.iap-kborn.de)). Since temperatures and densities were smoothed separately when producing these tables the altitude profiles at a given date are not exactly in hydrostatic equilibrium.

Temperatures are very low ( $<130$  K) at the high latitude polar summer mesopause from mid July (beginning of FS flights) until approximately end of August. The general thermal structure is similar to  $69^\circ\text{N}$  but there are also some differences explained in more detail below. The mesopause temperature decreases slightly from  $\sim 130$  K in mid-July to 126-128 K in late July/beginning of August. The mesopause altitude in summer is  $\sim 89$  km. Compared to FJL-JGR99 the mesopause temperature is very similar in mid-July but is significantly colder by 6–8 K in the second half of July and in August. Part of this difference (especially in late August) is due to the fact that the transition from summer to winter in Longyearbyen occurs later compared to Andøya. The mesopause altitude is higher by approximately 1 km at Longyearbyen compared to Andøya. At 82 km the temperature in summer is very close to 150 K, very similar to other Arctic and Antarctic stations. The temperatures in the upper mesosphere are significantly smaller compared to CIRA-1986 (see later) by up to 20 K. Assuming water vapor concentrations from *Körner and Sonnemann* [2001] there is an extended altitude range (82–92 km) with super-saturation (see Fig. 4 in *Lübken and Müllemann*, 2002).

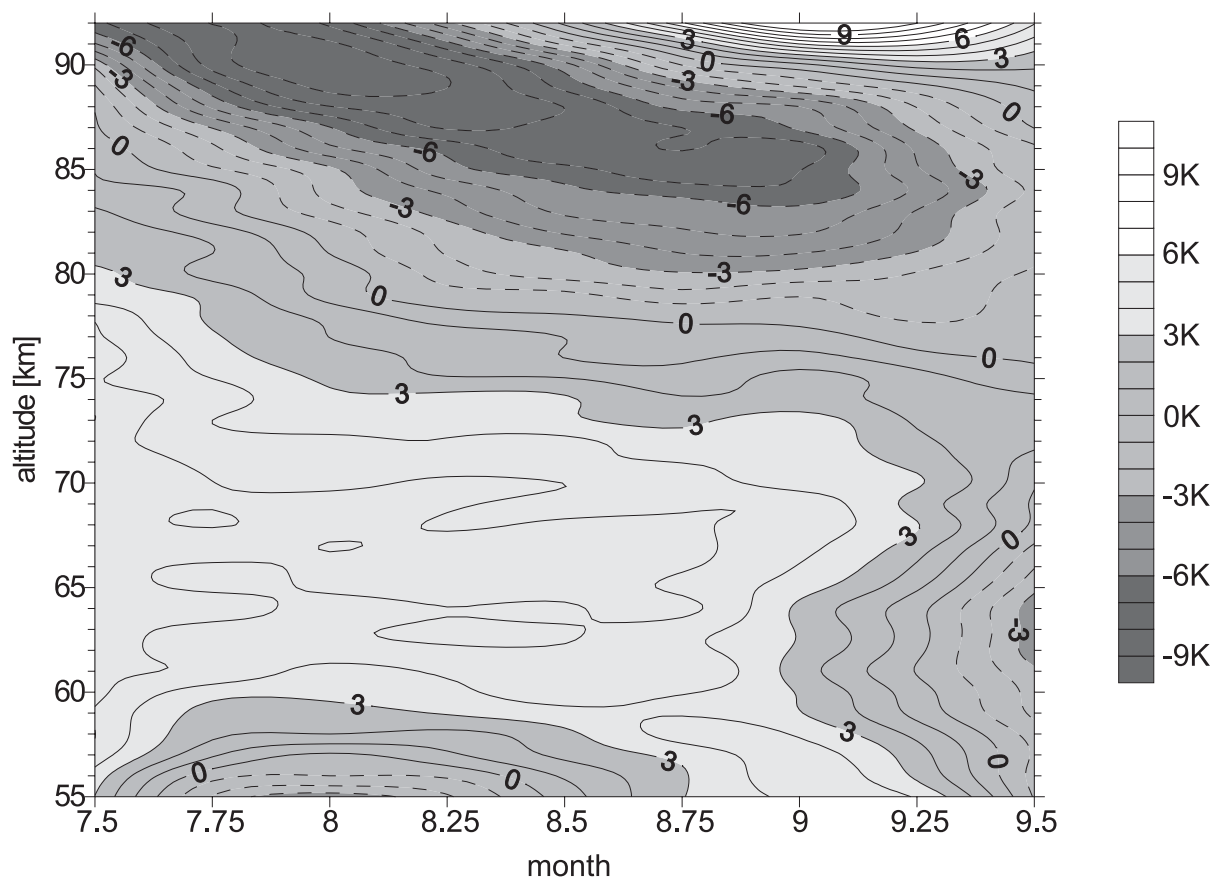


Fig. 2. Difference of FS temperatures obtained during ROMA compared with the climatology of FJL-JGR99 at  $69^\circ\text{N}$ . Negative (positive) values indicate smaller (larger) temperatures at Spitsbergen compared to Andøya.

## COMPARISON WITH OTHER MEASUREMENTS AND EMPIRICAL MODELS

### Temperatures

The difference of the ROMA temperatures to the FJL-JGR99 climatology at Andøya (69°N) is shown in Figure 2. Negative (positive) values indicate smaller (larger) temperatures at Spitsbergen compared to Andøya. As can be seen from this Figure the differences are surprisingly small (less than a few Kelvin) in the entire mesosphere, except for the mesopause region, where it is colder at Spitsbergen by up to 6–9 degrees compared to Andøya. This colder region is observed throughout the summer season until approximately the beginning of September and is most likely the cause of the different occurrence frequency of PMSE and NLC discussed later.

We now compare our results with empirical reference atmospheres taken from the Committee on Space Programs and Research (COSPAR) International Reference Atmosphere (CIRA) and from the latest thermospheric model based on mass spectrometer and incoherent scatter (MSIS) data, hereafter referred to as “CIRA-1986” and “MSIS-1990”, respectively [Fleming *et al.*, 1990; Hedin, 1991]. In Figure 3 we show temperature differences between our ROMA measurements and CIRA-1986. Negative (positive) values indicate smaller (larger) temperatures during ROMA compared to CIRA. During the entire campaign period from mid July until mid September and at heights above approximately 70–75 km temperatures are significantly smaller in our observations compared to the CIRA empirical model. The differences can be as large as –20 K at an altitude of approximately 82 km. Only at the very end of our campaign and at very high altitudes (above ~85–90 km) we find positive deviations.

In Figure 4 we present differences between FS temperatures and MSIS. Again, our observed temperatures are smaller in the upper mesosphere than the reference, but the difference is relatively small in mid July (–6 K) and increases with season in the upper mesosphere to values up to –16 K. In the lower mesosphere observed temperatures are somewhat larger compared to MSIS and CIRA.

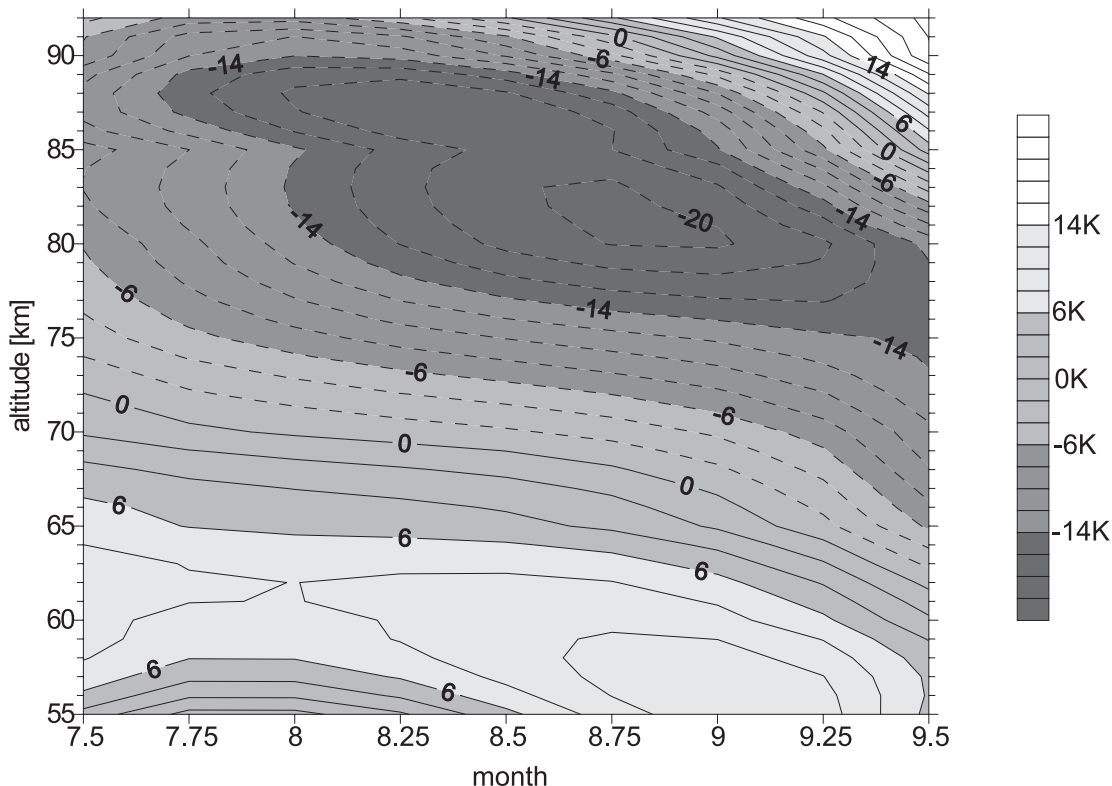


Fig. 3. Comparison of FS temperatures obtained during ROMA with CIRA-1986 at 80°N. Negative (positive) values indicate smaller (larger) temperatures during ROMA compared to CIRA.

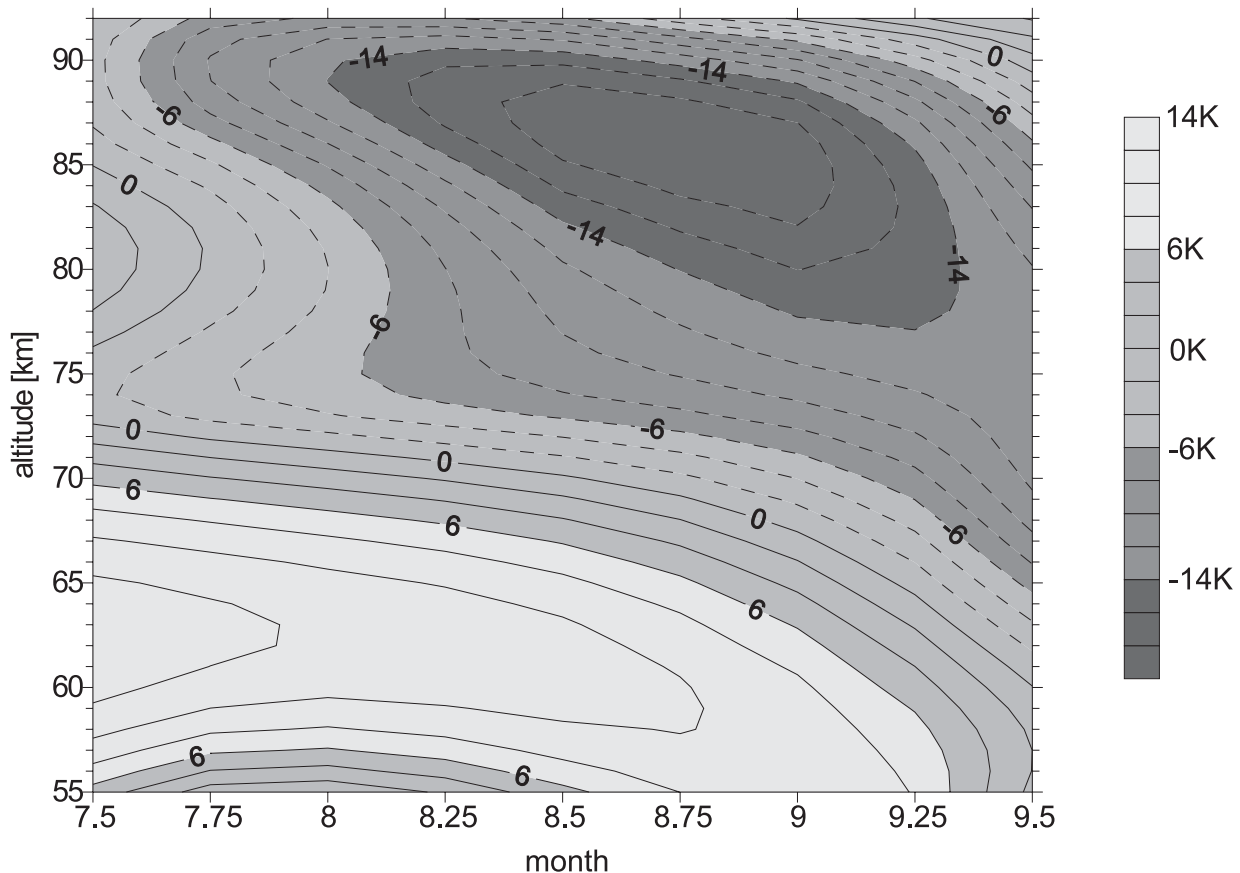


Fig. 4. Comparison of FS temperatures obtained during ROMA with MSIS at  $80^\circ\text{N}$ . Negative (positive) values indicate smaller (larger) temperatures during ROMA compared to MSIS.

### Densities

We have also compared mass densities derived from FS at Spitsbergen with measurements at other latitudes and with empirical models. A mass density profile is the prime quantity derived from the FS trajectory. Typical uncertainties are 2-3% below 90 km [von Zahn and Meyer, 1989]. In Figure 5 we show the relative mass density difference (in %) between Spitsbergen and Andøya. Negative values indicate smaller densities at Spitsbergen compared to Andøya. The differences are very small in the lower mesosphere (less than 1-2%) but range up to  $\pm 12\%$  in the upper mesosphere and the mesopause region. Here the differences are positive in summer and negative in the transition period.

In Figure 6 the relative mass density difference (in %) between Spitsbergen and CIRA-1986 is shown. Very large differences of up to -40% are observed in the upper mesosphere and lower thermosphere. This implies that the mass density in the real atmosphere is significantly less compared to the CIRA empirical model. This may have serious implications for various theoretical and practical applications (see below).

### WINDS

The lateral excursion of the falling sphere during descent measured by the tracking radar is used to determine horizontal winds. In Figure 7 we show individual profiles in the period from mid July to mid August. The mean zonal wind is negative (blowing towards the west) in the mesosphere in agreement with the climatological expectation. Typical zonal wind speeds are  $-(10-20)$  m/s, in rough agreement with CIRA-1986. They are considerably smaller compared to measurements at Andøya [Lübken *et al.*, 1990]. The meridional winds are weaker (typically +5 m/s) compared to the zonal component. We note from our compilation at Andøya that there is an apparently strong diurnal variation in the meridional wind

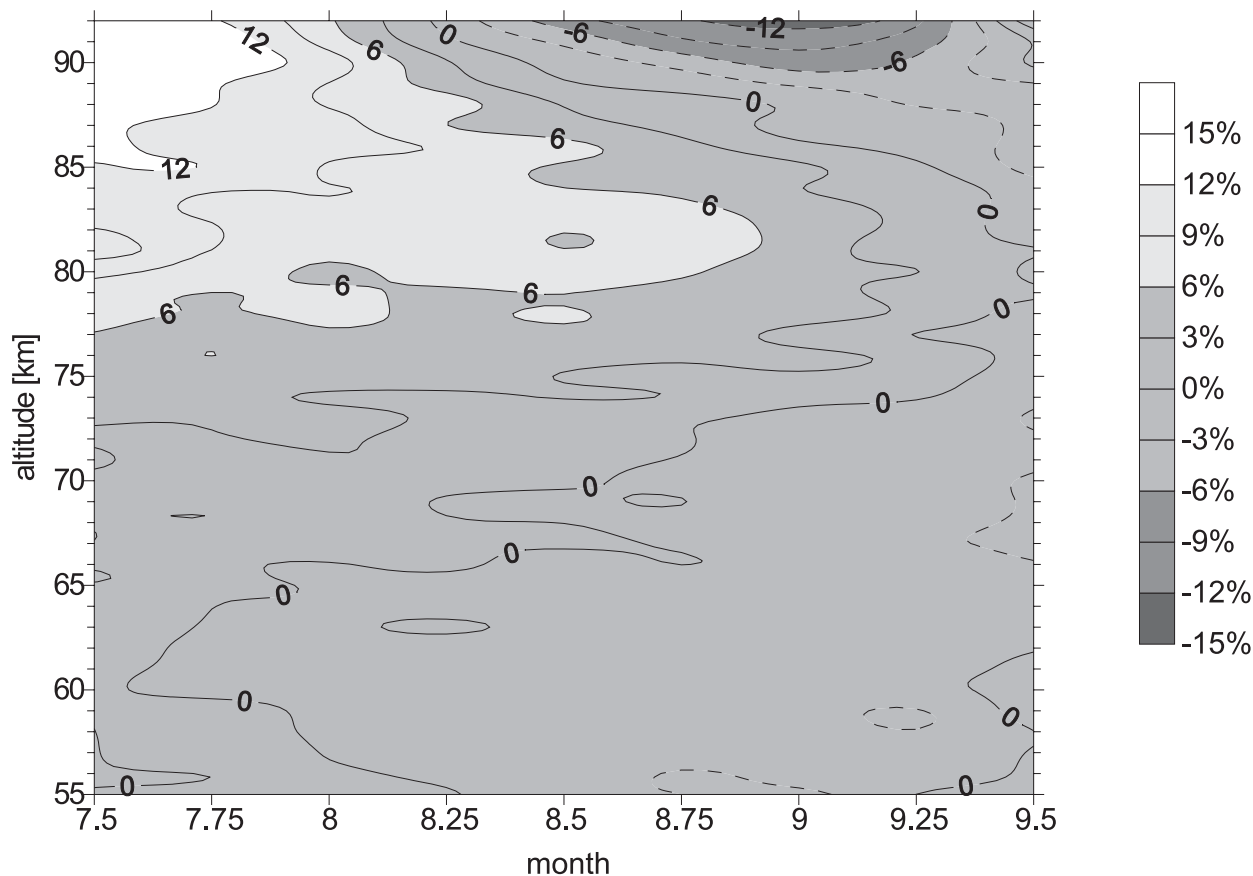


Fig. 5. Comparison of densities measured by FS during ROMA with the climatology of FJL-JGR99 at 69°N. Negative values indicate smaller densities at Spitsbergen compared to Andøya.

component in the mesosphere with mean southward winds around noon and mean northward winds around midnight (Müllemann, private communication). The small total number of flights in Spitsbergen does not allow to make a similar statement at this latitude.

## DISCUSSION AND SUMMARY

As has been shown above we find striking differences and similarities of temperatures, densities, and winds compared to other latitudes and to empirical models. These differences have interesting implications for our understanding of physical processes in the upper atmosphere and also practical applications when using remote sensing experimental techniques.

In the summer period (mid July to first part of August) the mesopause is  $\sim 0.9$  km higher at Longyearbyen compared to Andøya. We note that this difference is marginal taking into account the height resolution of the FS technique. The mesopause temperature difference is negligible in mid July but temperatures are approximately  $6\text{--}8^\circ\text{K}$  smaller at Longyearbyen compared to Andøya in the second half of July and in August. Part of this difference (especially in late August) is due to the later transition from summer to winter in Longyearbyen. We summarize that in the summer season the mesopause at  $78^\circ\text{N}$  is somewhat higher (by  $\sim 1$  km) and, at the end of the summer season, somewhat colder (by  $\sim 5\text{--}6^\circ\text{K}$ ) compared to  $69^\circ\text{N}$ . It is interesting to note that this variation of the summer mesopause altitude and temperature with latitude is also present in the IAP version of the Cologne Model of the Middle Atmosphere (COMMA/IAP) [Berger and von Zahn, 1999; von Zahn and Berger, 2003]. For midsummer conditions this model predicts a mesopause altitude increase by approximately 1 km per 10 degrees latitude and a corresponding mesopause temperature decrease by approximately  $8\text{--}10^\circ\text{K}$ , in general agreement with our observations.

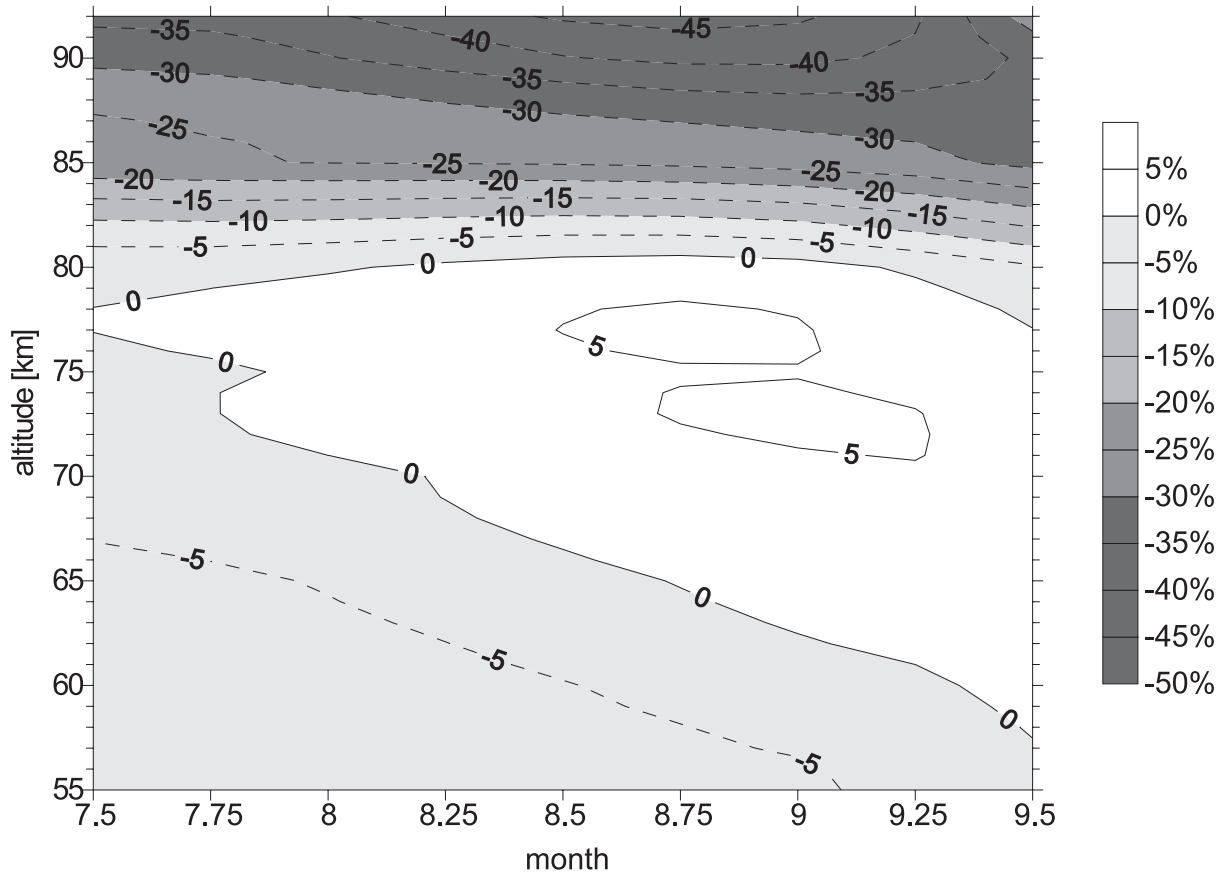


Fig. 6. Comparison densities measured by FS during ROMA with CIRA-1986 at 80°N. Negative values indicate smaller densities at Spitsbergen compared to CIRA.

Generally speaking one expects more and stronger NLC and PMSE when temperatures are smaller. Indeed, the occurrence rate of PMSE and NLC is larger at Longyearbyen compared to Andøya whereas the mean NLC altitude (83.4 km) is surprisingly similar at both sites [Rüster *et al.*, 2001; Höffner *et al.*, 2003]. We have noted earlier that the mesopause region is colder at higher latitudes, but at NLC heights the temperature difference is very small. Model studies are required to understand whether the similarities and differences in NLC and PMSE can be understood in terms of different background conditions.

A temperature difference between reality and empirical models of up to 20 degrees is very important when comparing general circulation models with measurements. This is also true for the observed density differences (up to almost 50%) which has also practical implications, for example when deriving concentrations from absolute number densities of trace gases, or when retrieving temperatures from meteor trail diffusion time constants [Hocking, 1999].

We expect that this new data set on the thermal and dynamical structure of the high latitude mesosphere will be used in future theoretical and experimental studies to improve our understanding of the main physical and chemical processes acting in this region and their importance for controlling the appearance of NLC and PMSE.

#### ACKNOWLEDGEMENTS

We thank Dr. Röttger and the SOUSY team for providing the PMSE profile shown in Figure 1. The excellent work by the crew of the Mobile Raketenbasis (DLR, Germany) and the Andøya Rocket Range is gratefully acknowledged. The ROMA project is supported by the Bundesministerium für Bildung, Wissenschaft, Forschung und Technologie, Bonn, under grants 50 OE 99 01 and 07 ATF 10 (AFO-2000).



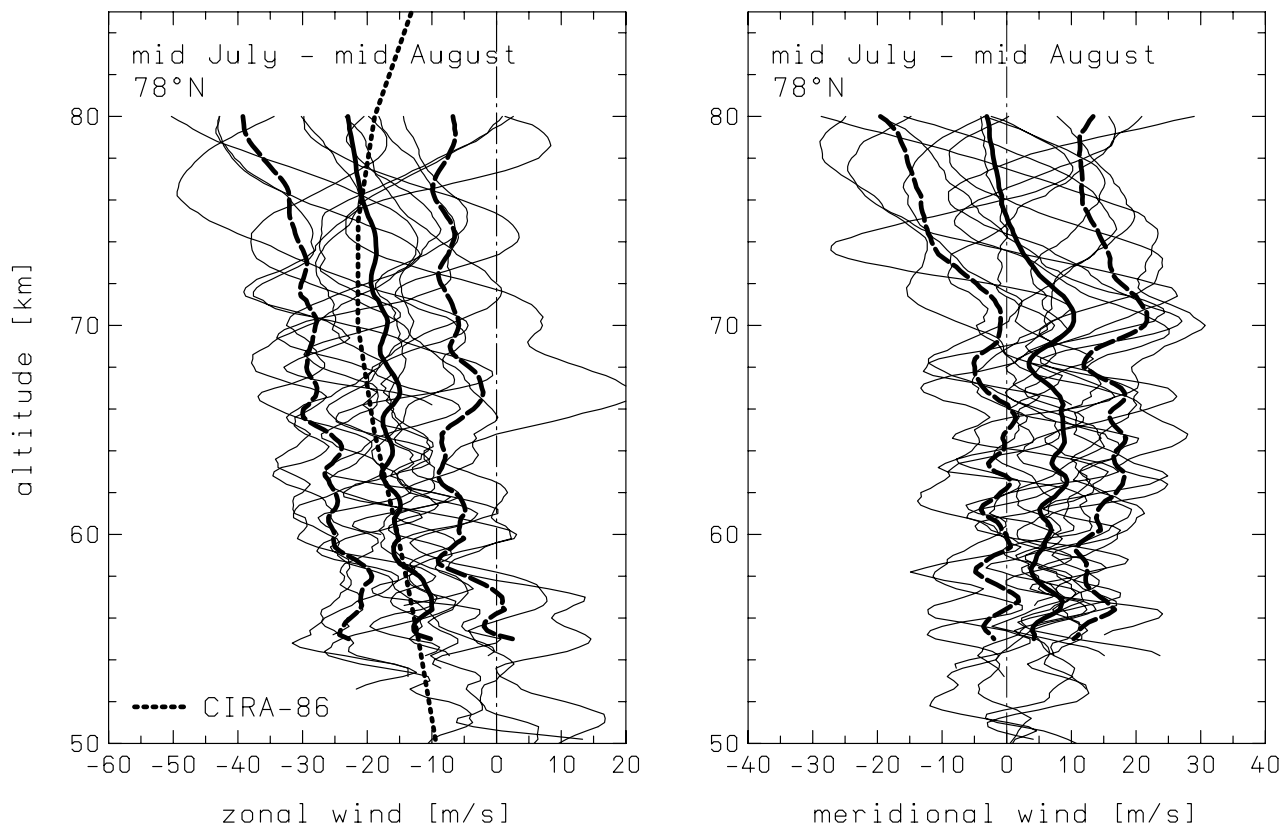


Fig. 7. Zonal (left panel) and meridional (right panel) winds derived from falling sphere flights from mid July to mid August. The mean profiles (thick lines) and the variability (thick dashed lines) are also shown. The dotted line indicates the zonal wind from CIRA-1986 which is taken as the average from July and August. There are no meridional winds in CIRA.

## REFERENCES

- Berger, U., and U. von Zahn, The two-level structure of the mesopause: A model study, *J. Geophys. Res.*, *104*, 22,083–22,093, 1999.
- Cho, J. Y. N., and J. Röttger, An updated review of polar mesosphere summer echoes: Observation, theory, and their relationship to noctilucent clouds and subvisible aerosols, *J. Geophys. Res.*, *102*, 2001–2020, 1997.
- Fleming, E. L., S. Chandra, J. J. Barnett, and M. Corney, Zonal mean temperature, pressure, zonal wind, and geopotential height as functions of latitude, *Adv. Space Res.*, *10*(12), 11–59, 1990.
- Gadsden, M., and W. Schröder, *Noctilucent clouds*, Springer-Verlag, New York, 1989.
- Hedin, A. E., Extension of the MSIS thermosphere model into the middle and lower atmosphere, *J. Geophys. Res.*, *96*, 1159–1172, 1991.
- Hocking, W. K., Temperatures using radar-meteor decay times, *Geophys. Res. Lett.*, *23*, 3297–3300, 1999.

- Höffner, J., C. Fricke-Begemann, and F.-J. Lübken, First observations of noctilucent clouds by lidar at Svalbard, *Atmos. Chem. Phys. Discuss.*, *3*, 521–549, 2003.
- Körner, U., and G. R. Sonnemann, Global 3D-modeling of the water vapor concentration of the mesosphere/mesopause region and implications with respect to the NLC region, *J. Geophys. Res.*, *106*, 9639–9651, 2001.
- Lindzen, R. S., Turbulence and stress owing to gravity wave and tidal breakdown, *J. Geophys. Res.*, *86*, 9707–9714, 1981.
- Lübken, F.-J., Thermal structure of the Arctic summer mesosphere, *J. Geophys. Res.*, *104*, 9135–9149, 1999.
- Lübken, F.-J., and A. Müllemann, First in-situ temperature measurements in the summer mesosphere at very high latitudes (78°N), *J. Geophys. Res.*, *in press*, doi:10.1029/2002JD002414, 2003.
- Lübken, F.-J., J. Höffner, C. Fricke-Begemann, A. Müllemann, M. Zecha, and J. Röttger, Mesospheric layers and temperatures at Spitsbergen, 78°N, in *Proceedings of the “Mesospheric Clouds” meeting*, edited by M. Gadsden and N. James, vol. 45 of *Memoirs of the British Astronomical Association*, pp. 97–114, British Astronomical Association, Burlington House, Piccadilly, London, W1J 0DU, U. K., 2002a.
- Lübken, F.-J., M. Rapp, and P. Hoffmann, Neutral air turbulence and temperatures in the vicinity of polar mesosphere summer echoes, *J. Geophys. Res.*, *107(D15)*, 4273, doi:10.1029/2001JD000915, 2002b.
- Lübken, F.-J., et al., Mean state densities, temperatures and winds during the MAC/SINE and MAC/EPSILON campaigns, *J. Atmos. Terr. Phys.*, *52*, 955–970, 1990.
- Lübken, F.-J., et al., Intercomparison of density and temperature profiles obtained by lidar, ionization gauges, falling spheres, datasondes, and radiosondes during the DYANA campaign, *J. Atmos. Terr. Phys.*, *56*, 1969–1984, 1994.
- Rapp, M., and F.-J. Lübken, On the nature of PMSE: Electron diffusion in the vicinity of charged particles revisited, *J. Geophys. Res.*, *108(D8)*, 8437, doi:10.1029/2002JD002857, 2003.
- Rapp, M., J. Gumbel, and F.-J. Lübken, Absolute density measurements in the middle atmosphere, *Ann. Geophys.*, *19*, 571–580, 2001.
- Rapp, M., F.-J. Lübken, A. Müllemann, G. E. Thomas, and E. J. Jensen, Small scale temperature variations in the vicinity of NLC: Experimental and model results, *J. Geophys. Res.*, *107(D19)*, 4392, doi:10.1029/2001JD001241, 2002.
- Rüster, R., J. Röttger, G. Schmidt, P. Czechowsky, and J. Klostermeyer, Observations of mesospheric summer echos at VHF in the polar cap region, *Geophys. Res. Lett.*, *28*, 1471–1474, 2001.
- Schmidlin, F. J., The inflatable sphere: A technique for the accurate measurement of middle atmosphere temperatures, *J. Geophys. Res.*, *96*, 22,673–22,682, 1991.
- von Zahn, U., and U. Berger, Freeze-drying at the summer polar mesopause: its likely persistence and consequences, *J. Geophys. Res.*, *in press*, doi:10.1029/2002JD002409, 2003.
- von Zahn, U., and J. Höffner, Mesopause temperature profiling by potassium lidar, *Geophys. Res. Lett.*, *23*, 141–144, 1996.
- von Zahn, U., and W. Meyer, Mesopause temperatures in polar summer, *J. Geophys. Res.*, *94*, 14,647–14,651, 1989.

E-mail of F.-J. Lübken: luebken@iap-kborn.de

Manuscript received 20 November 2002 ; revised 9 January 2003; accepted 10 January 2003.